Plant Soil (2016) 402:379–394
DOI 10.1007/s11104-015-2774-0

REGULAR ARTICLE

Integrated proteomics and metabolomics for dissecting the mechanism of global responses to salt and alkali stress in *Suaeda corniculata*

Qiuying Pang · Aiqin Zhang · Wei Zang · Lei Wei · Xiufeng Yan

Received: 29 October 2015 / Accepted: 8 December 2015 / Published online: 25 January 2016

Abstract
Background and aims Soil alkalinity and salinity are two of the most common environmental stress factors that impact plant growth and productivity. *S. corniculata* is native to the saline-alkali soil of Northeast China which shows a higher alkali tolerance than other *suaeda* plants. It will be very important to identify the effect of salt and alkali stress on *S. corniculata* through proteomics and metabolomics analysis to improve understanding of the resistance of plants.
Methods *S. corniculata* seedlings were exposed to salt and alkali stress for 72 h, respectively. Metabolic changes were quantified by conducting MS-based proteomics and NMR-based metabolomics analysis.
Results The response of *S. corniculata* to salt stress was distinct from that of plants subjected to alkali stress at both physiological and molecular levels. The integrated-omic studies identified 22 and 19 differentially expressed proteins and metabolites mainly involved in carbohydrate metabolism and amino acid metabolism.
Conclusions On account of the up-regulation of energy metabolism and higher accumulation of organic osmolytes, *S. corniculata* shows high pH resistance when it suffers alkali stress. These findings provide insights into the different regulatory mechanisms in halophyte *S. corniculata* response to salt and alkali stresses.

Keywords Salinity · Alkalinity · *Suaeda corniculata* · Proteomics · Metabolomics

Q. Pang and A. Zhang contributed equally to this work.

Responsible Editor: Frans J.M Maathuis.

Electronic supplementary material The online version of this article (doi:10.1007/s11104-015-2774-0) contains supplementary material, which is available to authorized users.

Q. Pang · A. Zhang · W. Zang · X. Yan (✉)
Alkali Soil Natural Environmental Science Center, Northeast Forestry University/Key Laboratory of Saline-alkali Vegetation Ecology Restoration in Oil Field, Ministry of Education, Harbin 150040, People's Republic of China
e-mail: xfyan@nefu.edu.cn

L. Wei
Key Laboratory of Coastal Zone Environmental Processes, Yantai Institute of Coastal Zone Research (YIC), Chinese Academy of Sciences (CAS), Shandong Provincial Key Laboratory of Coastal Zone Environmental Processes, YICCAS, Yantai 264003, People's Republic of China

Abbreviations

2-DE	Two dimensional electrophoresis
MALDI-TOF/TOF	Matrix-assisted laser desorption/ionization time-of-flight/time-of-flight
IAA	Iodoacetamide
RuBisCO	Ribulose bisphosphate carboxylase/oxygenase
GAPDH	Glyceraldehyde 3-phosphate dehydrogenase
TCA	Tricarboxylic acid
DTT	Dithiothreitol
ACN	Acetonitrile
TFA	Trifluoroacetic acid

Introduction

Soil salinization is one of the most common abiotic stressors to plant growth and productivity (Zhu 2001). Saline and sodic soils cover approximately 10 % of total arable lands and exist in over 100 countries (Wallender and Tanji 1990). For example, in the northeast of China, alkalinized grassland has exceeded 70 % (Kawanabe and Zhu 1991). Compared to salt stress, alkali stress adds the influence of high pH, which can inhibit uptake and disrupt the ionic balance of plant cells (Yang et al. 2007). With the increasing levels of soil salinization and alkalization worldwide, improving the salinity and alkali tolerance of plants is an important global priority, and in the near future it will be very important to identify strategies for improving the resistance of plants to salt and alkali stresses, so as to enable increasing the tolerance of crops to salt stress through the use of genetic engineering technologies.

Suaeda species are annual euhalophytes, among the most common plants in saline and alkaline soils, which are important halophyte resources with highly succulent leaves and able to accommodate ions without the need for secretion via salt glands and are widely distributed throughout the world (Shao and Li 1998; Flowers and Colmer 2008). More than twenty species of *Suaeda* have been reported for their ability to survive high salt conditions, including *S. salsa* (Zhang and Zhao 1998), *S. maritima* (Maathuis et al. 1992; Wetson and Flowers 2010), *S. aegyptiaca* (Askari et al. 2006), *S. asparagoides* (Ayarpadikannan et al. 2012), *S. fruticosa* (Khan and Ungar 1998), *S. glauca* (Yang et al. 2008b, *S. physophora* (Song et al. 2006) and *S. corniculata* (Wei et al. 2012). In particular, recent studies of salt responsive physiology, molecular genetics, proteomics and metabolomics in *S. salsa* have yielded more information for understanding the complex mechanisms of *Suaeda* plants' salt response and tolerance (Zhang et al. 2001; Lu et al. 2003; Pang et al. 2005; Han et al. 2011; Li et al. 2011, 2011b; Wu et al. 2012). In previous studies of *S. salsa*, salt treatment caused the up-regulation of aquaporin (Qi et al. 2009), vacuolar Na^+/H^+ antiporter (Qiu et al. 2007), V-ATPase and V-PPase (Wang et al. 2001), indicating that *Suaeda* can maintain homeostasis in water potential and ion distribution by increasing leaf succulence and compartmenting the ions. The choline monooxygenase (CMO) and betaine aldehyde dehydrogenase (BADH) genes in *S. salsa* which encode the enzymes involved in the synthesis of osmolytes were up-regulated under salt stress, suggesting that *Suaeda* plants could enhance their resistance to the osmotic stress by the accumulation of osmolytes when subjected to salt stress (Wu et al. 2012). In addition, salt stress accelerates the production of reactive oxygen species (ROS) in plant cells (Zhu 2001), and halophytes such as *Suaeda* species can maintain the balance between formation and removal of ROS by increasing the activity of antioxidant enzyme such as SOD (Wang et al. 2004; Guan et al. 2011), APX (Pang et al. 2005), GPX (Wu et al. 2012), and CAT (Pang et al. 2005; Wu et al. 2012).

As a member of the *Suaeda* genus, *S. corniculata* is native to the saline-alkali soil of Northeast China (Guan et al. 2010). *S. corniculata* shows a higher alkali tolerance than *S. salsa* and can survive in saline-sodic soil with pH ranged from 10 to 15.5 (Lu and Li 1994; Liu et al. 2011a). In this study, an integrated comparative proteomic and metabolomic approach was conducted identify the differentially expressed proteins and metabolites in *S. corniculata* under salt and alkali stresses, coupled with the analysis of protein function and metabolic pathways. This study is of prime interest to understand the underlying molecular mechanism of salt and alkali tolerance in *S. corniculata* and expand our knowledge of the metabolic processes by which *Suaeda* plants adapt to saline and alkaline soils.

Materials and methods

Plant material, growth conditions, stress treatment

Seeds of *S. corniculata* were collected from a saline-alkali soil area located in Zhaodong, Heilongjiang province, Northeast China. The seeds were soaked in distilled water for 2 h and sown in polyvinylchloride (PVC) cylinders filled with distilled water washed sand. Seedlings were grown in a greenhouse at 25/20 °C (day/night) with a 8 h light/16 h dark photoperiod, photosynthetically active radiation 150 $\mu mol \cdot m^{-2} \cdot s^{-1}$ and 50–70 % relative humidity and were irrigated daily by half strength Hoagland's solution (pH 6.21 ± 0.10). Four-week-old seedlings were transferred to hydroponic culture containers in half strength Hoagland's solution, which were changed daily, 12 plants were placed in each container filled with 1000 mL solution. After a week, the seedlings were treated with half strength Hoagland's solution containing 0, 100,150,

200, 300 mM NaCl (pH 6.12 ± 0.08) and 0, 50, 100, 150, 200 mM $NaHCO_3$ (pH 8.37 ± 0.15), the concentrations setting refer to previous studies on *S.salsa*, *S. maritime and S. glauca* (Flowers et al. 1976; Yang et al. 2008; Song et al. 2009). Five independent biological replicates were used in physiological analysis. After exposure for 72 h, the aboveground part of seedlings from control and exposed groups were randomly harvested and used for experiment, separately.

Measurement of biomass

Plants were harvested after exposure for 72 h and washed with distilled water, followed by surface drying with filter paper. After the determination of Fresh weights (FW), the samples were drying for 10 min in 105 °C and dried in an oven at 80 °C to a constant weight, and then dry weights (DW) was determined. Five plants of each treatment were independently carried out as biological replicates. One-way ANOVA was used to test the differences between control and each treatment followed by Tukey post hoc test. The differences were considered significant when $p < 0.05$.

Na^+, K^+ content analysis

Plants were harvested after exposure for 72 h and washed with distilled water, followed by surface drying with filter paper. The samples were oven-dried in an oven at 80 °C to a constant weight. Dry samples were homogenized by powdering and 20 mg of dry samples were treated with 1 ml 10 % nitric acid for 24 h. The extract was used to determine the contents of Na^+ and K^+ with flame atomic absorption spectrometer (AAS) (TAS-986, Beijing, China). Three replicates were used for each treatment. One-way ANOVA was used to test the differences between control and each treatment followed by Tukey post hoc test. The differences were considered significant when $p < 0.05$.

Proteomics analysis

Protein extraction

The proteins were extracted by the acetone/trichloroacetic acid method. Approximately 1 g fresh leaf tissue were harvested after exposure for 72 h from each treatment and ground into fine powder in liquid nitrogen. Three replicates were used for each treatment. The powder was precipitated in a 10 % (*w*/*v*) TCA, acetone solution containing 0.07 % (*v*/*v*) β-mercaptoethanol at −20 °C overnight. The mixture was centrifuged at 40,000 g at 4 °C for 1 h and the precipitates were washed with cold acetone containing 0.07 % (*v*/*v*) β-mercaptoethanol for three times. Pellets were dried by vacuum centrifuge and dissolved in 7 M urea, 2 M thiourea, 4 % (*w*/*v*) cholamidopropyl CHAPS, 40 mM dithiothreitol (DTT), 2 % (*v*/*v*) pharmalyte 4–7 (GE Healthcare, Waukesha, WI, USA), and 1 % (*v*/*v*) proteinase inhibitor (GE Healthcare, Waukesha, WI, USA) and shaked vigorously for 2 h at room temperature before being centrifuged at 40,000 g at 4 °C for 1 h. The subsequent supernatant was collected. The protein concentration was determined using the 2D Quant kit (GE Healthcare, Waukesha, WI, USA) with BSA as a standard. Sample were frozen in liquid nitrogen and kept at −80°Cuntil further use.

Two dimensional gel electrophoresis

Two dimensional electrophoresis of protein extracts was performed using a GE Healthcare 2-DE system according to the manufacturer's manuals. Each 1300 μg protein sample was loaded by rehydration to immobiline Dry Strips (pH 4–7 linear, 24 cm) (GE Healthcare, Waukesha, WI, USA). The separation on an IPGphor II unit (GE Healthcare, Waukesha, WI, USA) was performed with the following parameters: 30 V for 8 h, 50 V for 4 h, 100 V for 1 h, 300 V for 1 h, 500 V for 1 h, 1000 V for 1 h, and 8000 V for 12 h using hydration buffer (8 M urea, 2 % CHAPS, 20 mM DTT) containing 0.6 % (*v*/*v*) IPG buffer. After isoelectric focusing, the strips were equilibrated with 10 ml equilibration buffer I containing 6 M urea, 2 % SDS, 2.5 mM Tris-HCl (pH 8.8), 30 % glycerol, and 1 % DTT for 15 min, followed with 10 ml equilibration buffer II containing 6 M urea, 2 % SDS, 2.5 mM Tris-HCl (pH 8.8), 30 % glycerol, and 4 % 2-iodoacetamide (IAA) for 15 min. The second dimension separation of proteins was performed on SDS-PAGE gel (12.5 % polyacrylamide) using Ettan™ Daltsix apparatus (GE Healthcare, Waukesha, WI, USA). The electrophoresis was carried out at 25 °C and 3.5 w/gel for 30 min and then 17.5 w/gel for 4.5 h until the bromophenol blue dye front arrived at the bottom of the gels.

Image and statistical analysis

Proteins were visualized by coomassie brilliant blue R250 staining, and gel images were acquired using an ImageScanner (GE Healthcare, Waukesha, WI, USA). Image analysis was performed with ImageMaster 2D Platinum Software Version 7.0 (GE Healthcare, Waukesha, WI, USA). After automated detection and matching, manual editing was carried out to correct the mismatched and unmatched spots. Spots were considered reproducible when they were well resolved in the three biological replicates. For each matched spot, a measurement was carried out for each biological replicate, and normalized volumes were computed using the total spot volume normalization procedure of the software. The normalized volume of each spot was assumed to represent its expression abundance. A criterion of $p < 0.05$ and an abundance ratio of at least 2.0 were used to define significant differences when analyzing parallel spots between groups with two-way ANOVA.

In-gel digestion and MALDI-TOF/TOF analysis

Selected spots were excised from 2D gels, washed with sterile deionized water, and digested with trypsin as described previously (Chen et al. 2011). For MALDI-TOF/TOF MS analysis, tryptic peptides were desalted with C18 Ziptips (Millipore) and spotted onto a MALDI plate by mixing 1:1 with the matrix solution (1 % a-cyano-4-hydroxy-trans-cinnamic acid in 60 % ACN containing 0.1 % TFA). MS/MS spectra were acquired using a 4800 MALDI-TOF/TOF mass spectrometer (Applied Biosystems/MDS Sciex, USA). The peptide MS/MS spectra were searched against NCBI nonredundant fasta database (8,224,370 entries, downloaded on April 14, 2009) using MASCOT search engine (http://www.matrixscience.com). Mascot was set up to search green plants only, assume trypsin digestion and one allowed miscleavage. The mass tolerance for both parent ion and fragment ion mass was set to be 0.3 Da. Iodoacetamide derivatization of Cys, deamidation of Asn and Gln, and oxidation of Met were specified as variable modifications. Unambiguous identification was judged by the number of peptides, sequence coverage, MASCOT MOWSE score and the quality of MS/MS spectra.

For the proteins identified by MASCOT, their accession numbers were directly searched against the NCBInr database (http://blast.ncbi.nlm.nih.gov/) to obtain the proteins corresponding blast information. Non-commercial databases, KEGG (http://www.genome.jp/kegg/pathway.html), were utilized to search for protein functional classification.

Metabolomics analysis

Metabolite extraction

Polar metabolites were extracted from the leaves of *S. corniculata* using the solvent system of methanol/water (1/1), as described previously (Wu et al. 2011). Six replicates were used for each treatment. The fresh leaf tissue (approximately 100 mg) was ground in liquid nitrogen with a mortar and pestle. The tissue powder was transferred to a tube containing approximate 50 ceramic beads with 1 mm diameter and homogenized in 3.33 ml g^{-1} methanol/water (1/1). After vortex mixing for 15 s three times, the homogenate was centrifuged at 3000 × g for 10 min at 4 °C, the supernatant was removed and then lyophilized. It was subsequently resuspended in 600 μL phosphate buffer (0.1 M Na_2HPO_4 and NaH_2PO_4, including 0.5 mM TSP, pH 7.0) in D_2O. Before being centrifuged at 3000 g for 5 min at 4 °C, the mixture was vortexed for 15 s, and then the supernatant substance (550 μL) was pipetted into a 5 mm NMR tube for following NMR analysis.

NMR analysis

Extraction analysis of *S. corniculata* leaf tissue was performed with a Bruker AV 500 NMR spectrometer at 500.18 MHz (at 298 K) (Wu et al. 2012). One dimensional (1D) ^{1}H NMR spectra were obtained with the following parameters: 11.9 μs pulse, 6009.6 Hz spectral width, 0.1 s mixing time, and 3.0 s relaxation delay with standard 1D NOESY pulse sequence, with 128 transients collected into 16,384 data points. Datasets were zero-filled to 32,768 points, and exponential line-broadenings of 0.3 Hz were applied prior to Fourier transformation.

Data processing and statistical analysis

All ^{1}H NMR spectra were phased, baseline-corrected, and calibrated (TSP at 0.0 ppm) using TopSpin (version 2.1, Bruker). Metabolites were assigned and quantified following the tabulated chemical shifts (Wu et al. 2011, 2013; Ji et al. 2013) and using the software Chenomx

(Evaluation Version, Chenomx Inc., Canada). We used principal components analysis (PCA) in this work for the separation of control and different salt exposed groups. PCA is an exploratory unsupervised pattern recognition (PR) method that calculates inherent variation within the data sets without use of the class membership. The algorithm of PCA calculates the highest amount of correlated variation along principal component (PC1), with subsequent PCs containing correspondingly smaller amounts of variance. For each model built, the loading vectors for the PCs could be used for the identification of the contributive metabolites (metabolic biomarkers) for the clusters (Xu 2004). Data were statistically analyzed using SPSS 13.0. All of the treatments were replicated six times, means and calculated standard deviation (SD) were reported. For test statistical significance ($p < 0.05$ and $p < 0.01$) of separations between the control and treated groups, Tukey HSD-test was performed of different samples.

Result

Plant growth response to NaCl and $NaHCO_3$ stress

At low concentrations NaCl and $NaHCO_3$ treatment, *S. corniculata* was fresh and green, but it showed severe wilting and tended to be unwell at 300 mM NaCl and 200 mM $NaHCO_3$ treatment. FW of *S. corniculata* were decreased slightly at 100 mM NaCl, but decreased markedly with increasing NaCl concentrations under salt stress (Fig. 1a). With increasing $NaHCO_3$ concentrations, the FW of *S. corniculata* decreased significantly (Fig. 1b). DW of *S. corniculata* were decreased slightly by both NaCl and $NaHCO_3$ stress (Fig 1). Under 300 mM NaCl and 200 mM $NaHCO_3$ treatment, the stress reduced the FW of *S. corniculata* by 55.7 % and 61.7 %, respectively, and reduced the DW of *S. corniculata* by 39.1 % and 31.9 %, respectively. Given this evidence that, 300 mM NaCl and 200 mM $NaHCO_3$ have severe shock effects on plants, 150 mM NaCl and 150 mM $NaHCO_3$ were selected as the salt and alkali stress for 2-DE and metabolic analysis.

Effects of NaCl and $NaHCO_3$ stress on Na^+, K^+ content

The Na^+ contents of *S. corniculata* increased with increasing salinity and alkali levels under both NaCl and $NaHCO_3$ stresses (Fig. 2). K^+ contents were much lower than in the controls at the lowest dose of both stresses, and decreased with increasing NaCl treatment intensity, but did not change obviously under $NaHCO_3$ stress with increasing alkalinity (Fig. 2). The K^+/Na^+ ratios of *S. corniculata* under NaCl and $NaHCO_3$ treatment were much lower than in the controls, whereas the changes in the K^+/Na^+ ratio under NaCl stress were much higher than under $NaHCO_3$ stress.

Comparative proteome analysis

Four-week-old seedlings of *S. corniculata* were treated with 150 mM NaCl and 150 mM $NaHCO_3$ for 72 h. To investigate the temporal changes of protein profiles in response to NaCl and $NaHCO_3$ stress, 2-DE gels from three biological replicates were analyzed to detect proteins extracted from the leaves of control and treated seedlings (Fig. 3, Supplementary Figure S1 and S2). More than 1000 protein spots were reproducibly detected on gels by the Melanie 7.0 software. The data showing significant difference between control and treatment at 0.05 level were considered up- or down-regulated protein spots. Quantitative image analysis revealed that a total of 30 protein spots changed significantly in abundance (Vol%) by >2.0-fold. MALDI-TOF/TOF MS analysis of these spots was successfully performed, and the mass spectra were searched against the NCBInr database using the Mascot search engine. In total, 22 proteins were successfully identified from the 30 differentially expressed protein spots and are listed in Tables 1 and 2 (Supplementary Table S3). Among the 22 proteins, 10 proteins were observed as being differentially expressed under NaCl treatments and 12 proteins under $NaHCO_3$ treatments (Fig. 3a). In addition, the expression abundance of one protein was modulated both by NaCl and $NaHCO_3$ treatments, but it shows different regulation patterns under the two types of salt stress. According to KEGG pathway analysis of the protein cell function categories, the functions of these proteins could be classified into seven groups including carbohydrate metabolism, energy metabolism, photosynthesis, nucleotide metabolism, protein synthesis, stress and defense, and unknown (Fig. 4).

All of the differentially expressed proteins that responded to NaCl stress revealed a relatively decreased abundance in *S. corniculata*. Only a small portion of these identified proteins were induced by $NaHCO_3$ treatments. We found that three of them, namely RuBisCO large subunit-binding protein (spot 572) and

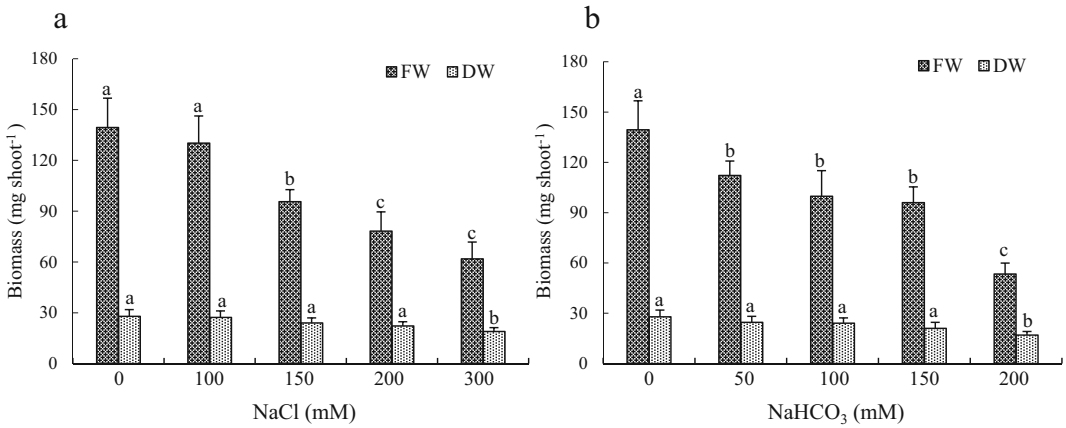

Fig. 1 Effects of NaCl and $NaHCO_3$ on *S. corniculata* growth. Five-week-old seedlings were treated without stressors (control) or with 100, 150, 200, 300 mM NaCl or 50, 100, 150, 200 mM $NaHCO_3$. (**a**) Fresh and dry weight were measured 72 h after the start of NaCl treatment. (**b**) Fresh and dry weight were measured 72 h after the start of $NaHCO_3$ treatment. *Error bars* show the SE for three biological replicates. Significant differences ($p < 0.05$ by one-way ANOVA analysis) are indicated by different letters

chloroplast RNA binding protein (spot 1008), which functions in photosynthesis, and ATP-dependent zinc metalloprotease (spot 642), which is correlated to protein processing, showed significant increases in their expression abundance.

Metabolic response

Through proteomics analysis, we have observed many differentially expressed proteins involved in various cellular metabolism pathways. To gain more insights into the modulation of metabolic processes in the *S. corniculata* response to salt and alkali stress, NMR analysis was conducted to detect the metabolic changes between the control and treated samples with 150 mM NaCl and 150 mM $NaHCO_3$ for 72 h. A representative ^{1}H NMR spectrum of the leaves of *S. corniculata* extracts is shown in Fig. 5 (Supplementary Figure S4). PCA results from the analysis of NMR spectral data showed alkali-exposed samples were clearly separated from control and salt-exposed samples along PC1 axis ($p < 0.05$) from the PC scores plot (Supplementary Figure S5). A total of 19 metabolites were identified in the leaves of *S. corniculata* involved in various metabolite classes, including nine amino acids (valine, glycine, alanine, leucine, isoleucine, glutamine, glutamate, aspartate and threonine), three energy storage compounds (sucrose, glucose and fructose), four intermediates in the tricarboxylic acid (TCA) cycle (malate, succinate, 2-oxoglutarate, and fumarate), one organic

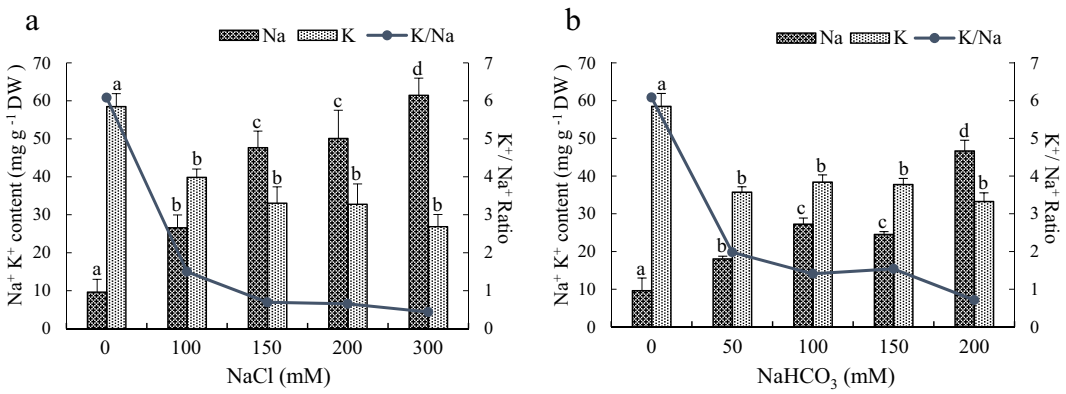

Fig. 2 Effects of (**a**) NaCl and (**b**) $NaHCO_3$ stresses on Na^+ and K^+ concentrations and K^+/Na^+ in *S. corniculata*. Seedlings were treated with 0, 100, 150, 200, 300 mM NaCl or 50, 100, 150, 200 mM $NaHCO_3$. *Error bars* show the SE for three biological replicates. Significant differences ($p < 0.05$ by one-way ANOVA analysis) are indicated by different letters

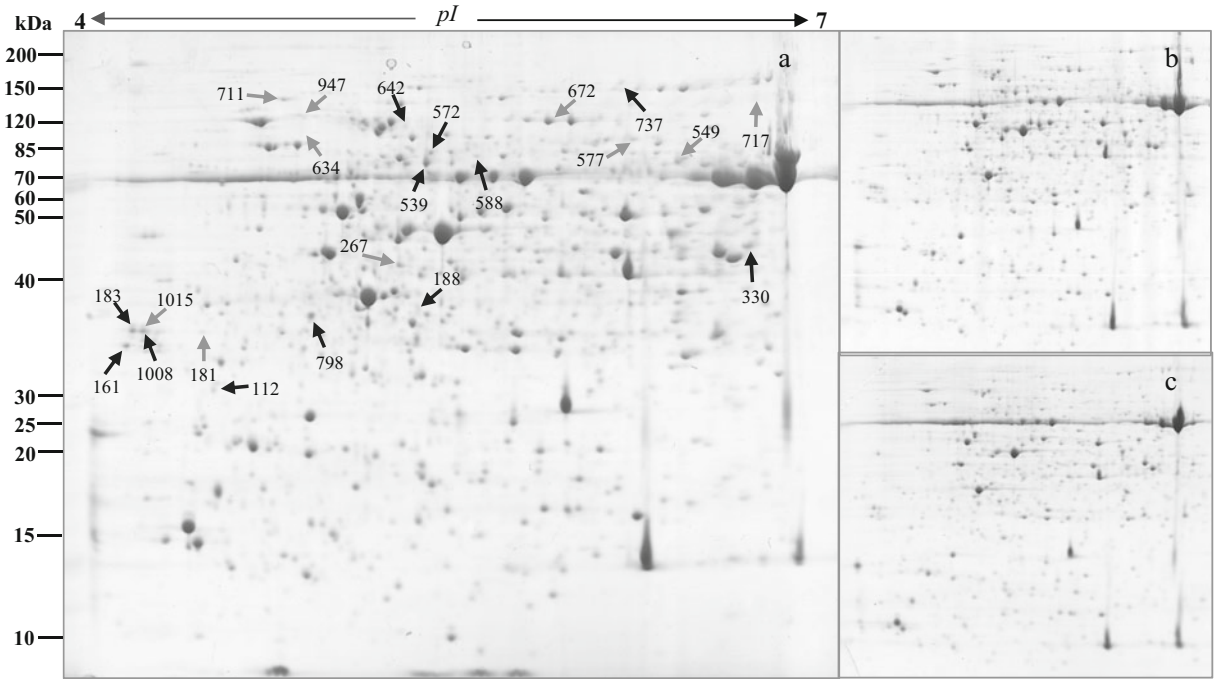

Fig. 3 Representative 2-DE gels of protein samples from *S. corniculata* under salt and alkali stresses. (**a**) A total of 22 statistically significant differential spots are labeled with arrows. *Gray and black arrows* indicate salt and alkali response protein spots, respectively. (**b**) NaCl- and (**c**) $NaHCO_3$-treated samples

osmolyte (betaine) and others (dimethylamine and choline) (Fig. 6). Except sucrose and alanine, the other metabolites exhibited no significant differences under NaCl stress. Among the rest of these metabolites, only betaine displayed up-regulated abundance and the remaining 15 metabolites were down-regulated after NaCl treatment. In contrast, 11 of 19 metabolites were significantly changed under $NaHCO_3$ stress. Almost all of these metabolites were up regulated by $NaHCO_3$ treatment, and only one metabolite (sucrose) was down-regulated. Compared with the metabolic expression of *S. corniculata* under NaCl stress, 16 of 19 metabolites (except sucrose, threonine and dimethylamine) showed significant up-regulation in $NaHCO_3$-treated plants (Fig. 6).

Discussion

Comparing alkali stress with salt stress, the high pH environment that surrounds the plant root can cause the precipitation of metal ions and phosphorus, greatly affecting the absorption of inorganic anions and disrupting the ionic balance and pH homeostasis in plant tissues (Shi and Zhao 1997; Yang et al. 2007, 2008c). It is understood that currently, only a few plant species of alkali-resistant halophytes can survive in saline and alkaline land (Zheng and Li 1999; Yang et al. 2008a). In our study, under 150 mM $NaHCO_3$ and NaCl conditions, the fresh weight of *S. corniculata* declined slightly, the plants responded to alkali and salt stress by a significant inhibition of growth with increasing concentration treatment, and the phenotype changes caused by $NaHCO_3$ stress were more obvious than the results of NaCl stress. These results indicated that the injurious effects of alkali stress on the growth of *S. corniculata* were more severe than for salt stress, which was consistent with previous reports (Li et al. 2009; Guo et al. 2009).

Under salt stress, Na^+ competes with K^+ for uptake into plant roots through the high affinity K^+ transporter and non-selective cation channels (Munns 2002; Munns and Tester 2008). The Na^+ contents of *S. corniculata* increased with increasing salinity and alkali levels under both NaCl and $NaHCO_3$ stresses (Fig. 2), but Na^+ accumulation in $NaHCO_3$-treated plants was lower than in NaCl-treated plants. It is suggested that alkali stress may attributable to an inhibitory effect of high pH on the absorption of inorganic anions (Munns and Tester

Table 1 Proteomics responses to salt stress in *S. corniculata*

Spot No.[a]	NCBI Accession No. (GI)[b]	Protein Name	Species	Thero kD/pI[c]	Score[d]	Sequence coverage(%)[e]	Peptides matched[f]	Fold changes	*p*-Value
Carbohydrate metabolism									
672	gi|194,396,261	plastid transketolase	*Nicotiana tabacum*	6.16/80.5	288	8	6	−3.52	0.05
549	gi|255,540,719	aldehyde dehydrogenase	*Ricinus communis*	7.14/58.7	130	4	2	−3.42	0.03
Photosynthesis									
267	GT153021	plate-7-A2-M13F Chlorenchyma cells of Bienertia sinuspersici Bienertia sinuspersici cDNA 5'	*Bienertia sinuspersici*	8.97/43.6	254	12	3	−6.83	0.01
1015	gi|168,274,276	chloroplast RNA binding protein	*Mesembryanthemum crystallinum*	4.68/33.8	640	38	9	−2.90	0.04
Nucleotide metabolism									
577	gi|224,144,020	predicted protein	*Populus trichocarpa*	6.25/58.7	122	7	3	−5.16	0.02
Protein synthesis, folding and destination									
181	BI095874	serine carboxypeptidase	*Beta vulgaris*	4.73/26.5	91	7	2	−3.34	0.03
717	gi|309,756,515	pollen allergen MetE	*Amaranthus retroflexus*	6.12/84.0	304	9	5	−8.59	0.02
Stress and defense									
949	gi|115,467,076	Os06g0215300	*Oryza sativa Japonica Group*	5.34/75.8	100	4	2	−4.26	0.04
711	gi|260,505,494	heat shock protein 90	*Ipomoea nil*	4.92/90.6	314	6	4	−2.71	0.05
unknown									
634	BQ594018	BQ594018 E012759-024-025-F15-SP6 MPIZ-ADIS-024-developing root Beta vulgaris cDNA clone 024–025-F15 5-PRIME	*Beta vulgaris*	4.34/18.9	82	8	1	−2.66	0.05

[a] Assigned spot number as indicated in Fig. 3

[b] Database accession numbers according to NCBInr

[c] Theoretical mass (kDa) and pI of identified proteins. Theoretical values were retrieved from the protein database

[d] Mascot score reported after searching against the NCBInr database

[e] The percentage of sequence coverage

[f] Number of peptides sequenced

Table 2 Proteomics responses to alkali stress in *S. corniculata*

Spot No.[a]	NCBI Accession No. (GI)[b]	Protein Name	Species	Thero kD/pI[c]	Score[d]	Sequence coverage(%)[e]	Peptides matched[f]	Fold changes	*p*-Value
Carbohydrate metabolism									
188	gi|255,540,407	2-deoxyglucose-6-phosphate phosphatase	*Ricinus communis*	7.92/35.0	206	14	5	−3.22	0.03
330	gi|18,076,100	glyceraldehyde-3-phosphate dehydrogenase	*Marchantia polymorpha*	8.14/42.8	363	10	6	−3.05	0.03
737	gi|22,633	fructose-bisphosphate aldolase	*Spinacia oleracea*	7.57/42.7	78	5	2	−2.95	0.04
Photosynthesis									
572	gi|2,493,650	RuBisCO large subunit-binding protein subunit beta	*Secale cereale*	4.88/53.7	282	11	3	2.36	0.02
183	gi|168,274,276	chloroplast RNA binding protein	*Mesembryanthemum crystallinum*	4.68/33.8	576	33	8	−4.29	0.00
1008	gi|168,274,276	chloroplast RNA binding protein	*Mesembryanthemum crystallinum*	4.68/33.8	640	38	9	3.61	0.00
Energy metabolism									
539	gi|306,485,977	atpA	*Davidia involucrata*	5.27/55.6	636	20	9	−6.42	0.01
588	gi|7,636,090	ATPase subunit I	*Spinacia oleracea*	5.47/47.3	106	9	3	−9.38	0.04
Protein synthesis, folding and destination									
642	gi|75,114,857	ATP-dependent zinc metalloprotease FTSH 2	*Oryza sativa Japonica Group*	5.54/72.6	606	15	8	2.73	0.05
798	gi|225,443,260	hypothetical protein	*Vitis vinifera*	5.17/31.6	127	7	2	−2.60	0.05
Stress and defense									
112	gi|15,222,089	pathogenesis-related protein 5	*Arabidopsis thaliana*	4.75/26.1	58	5	1	−2.31	0.01
unknown									
161	gi|118,481,688	unknown	*Populus trichocarpa*	4.34/22.3	230	20	4	−4.43	0.02

[a] Assigned spot number as indicated in Fig. 3

[b] Database accession numbers according to NCBInr

[c] Theoretical mass (kDa) and pI of identified proteins. Theoretical values were retrieved from the protein database

[d] Mascot score reported after searching against the NCBInr database

[e] The percentage of sequence coverage

[f] Number of peptides sequenced

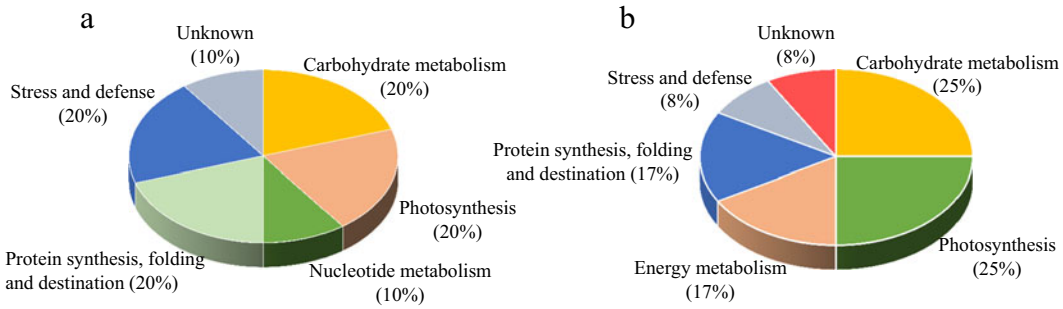

Fig. 4 Functional classification of differentially expressed proteins identified in *S. corniculata* under salt and alkali stresses. (**a**) Protein categories of seedlings under NaCl stress. (**b**) Protein categories of seedlings under $NaHCO_3$ stress

2008). The converse situation in K^+ contents change mode under NaCl stress, it decreased with increasing NaCl treatment intensity. In the $NaHCO_3$-treated plants in our study, the K^+ contents were clearly lower than control, but did not change significantly with increasing alkalinity (Fig. 2b). These results were consistent with the analysis of the responses of the alkali-resistant halophytes *S. glauca* and *Puccinellia tenuiflora* to salt and alkali stresses (Yang et al. 2008b; Guo et al. 2010). It should be emphasized that the K^+ contents did not change significantly between different level alkali stresses, which indicated that there might be no competitive inhibition between Na^+ and K^+ absorption in *S. corniculata* under alkali stress, suggesting that this plant might have a unique pathway of Na^+ absorption independent of the K^+ pathway, and that separation might be related to the resistance of alkali stress in *S. corniculata*.

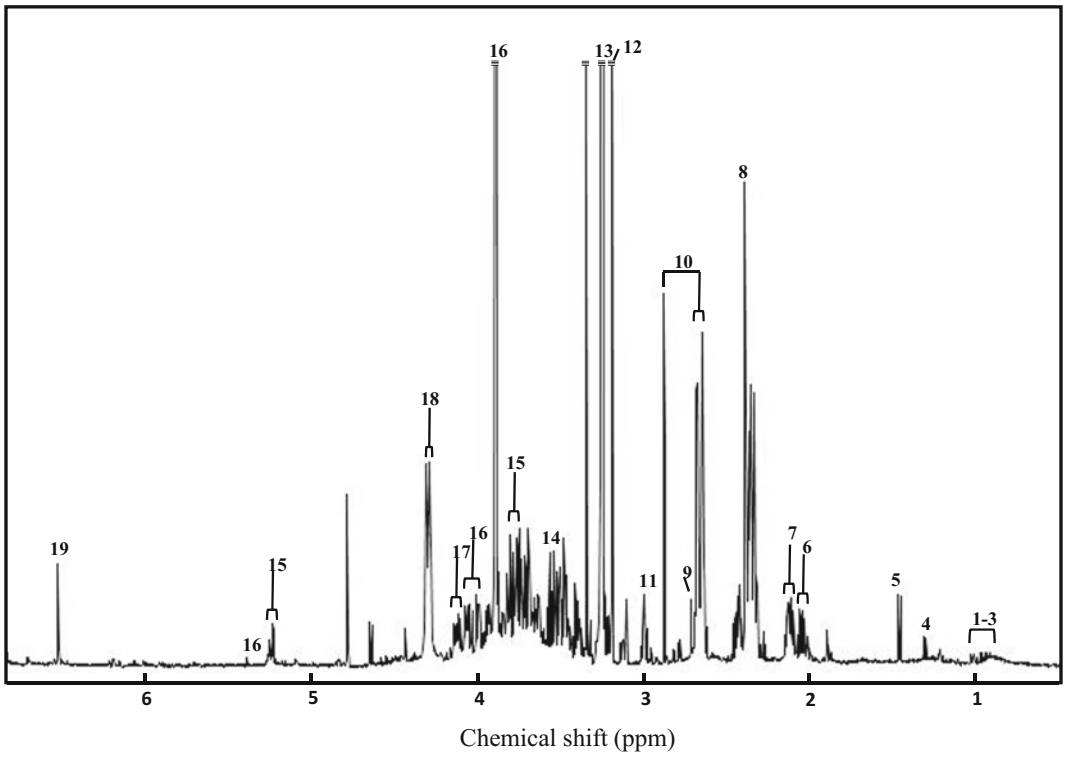

Fig. 5 A representative ^{1}H-NMR spectrum of the metabolites identified in *S. corniculata*. (*1*) valine, (*2*) isoleucine, (*3*) leucine, (*4*) threonine, (*5*) alanine, (*6*) glutamate, (*7*) glutamine, (*8*) succinate, (*9*) dimethylamine, (*10*) aspartate, (*11*) 2-oxoglutarate, (*12*) choline, (*13*) betaine, (*14*) glycine, (*15*) glucose, (*16*) sucrose, (*17*) fructose, (*18*) malate, (*19*) fumarate

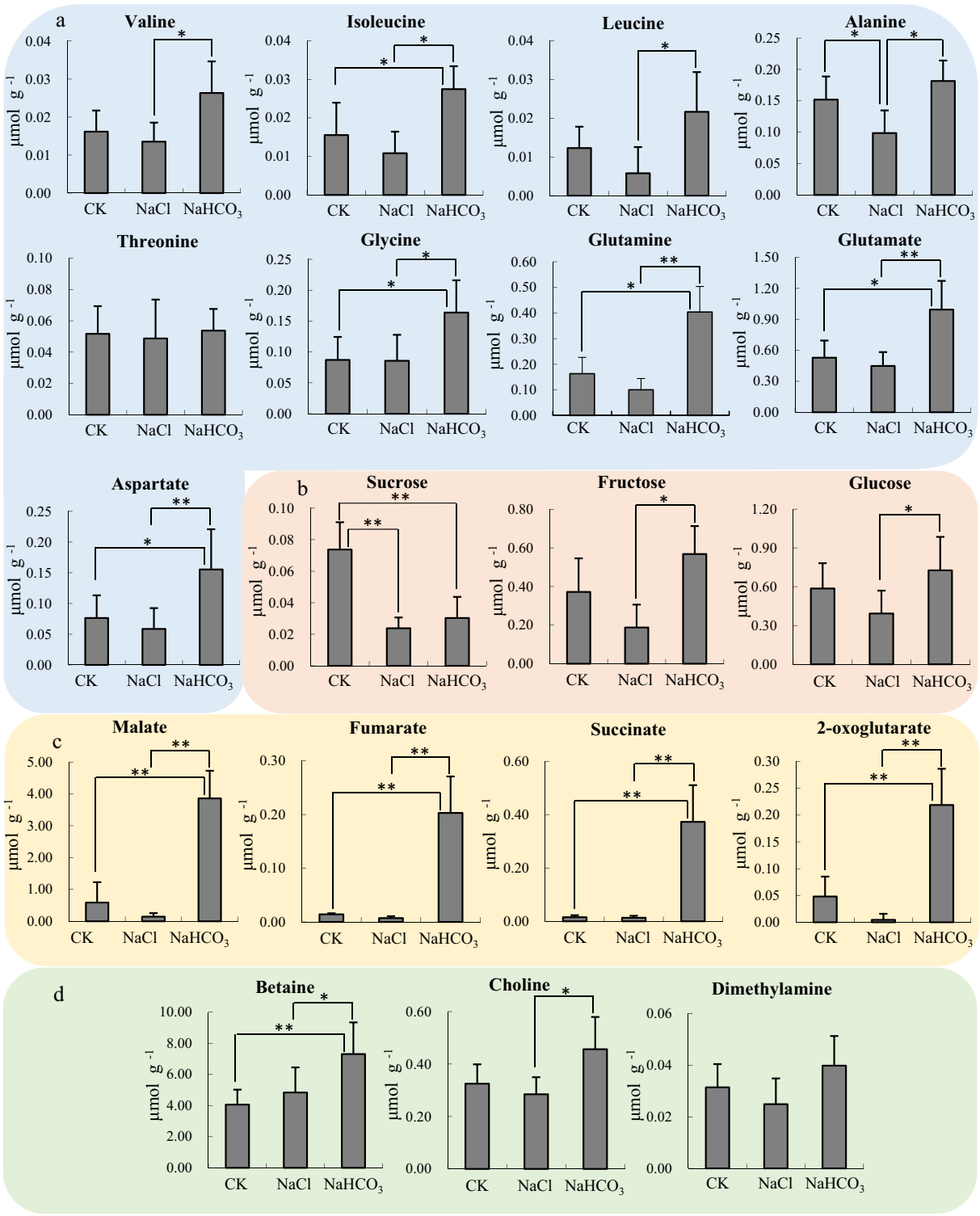

Fig. 6 Metabolomic responses to salt and alkali stresses in *S. corniculata*. (**a**) The response of metabolites of amino acids, (**b**) sugars, (**c**) intermediates of the TCA cycle, (**d**) osmolytes and others. Significant differences ($p < 0.05$ and $p < 0.01$ by Tukey HSD-test) are indicated by one or two asterisks

To gain insight into the proteomic and metabolomic responses of *S. corniculata* towards alkalinity and salinity, we identified some differently expressed proteins and metabolites involved in a variety of cellular processes, mainly including carbohydrate metabolism, energy metabolism, photosynthesis, protein synthesis, stress and defense. A better understanding of these analysis data may help to determine the global responses to salt and alkali stresses in *S. corniculata* based on the modulation of certain key biological processes by salinity and alkalinity.

Carbohydrate metabolism

Based on our observations, two metabolizing enzymes, aldehyde dehydrogenase (spot 549) and plastid transketolase (spot 672), involved in the glycolysis and pentose phosphate pathways were down-regulated under salt stress. Transketolase catalyzes reactions in the oxidative pentose phosphate pathway and produces erythrose-4-phosphate, which is a precursor for the shikimate pathway leading to the phenylpropanoid metabolism (Henkes et al. 2001). It has previously been reported that plastid transketolase exhibits opposite expression patterns in glycophytes and halophytes under salt stress (Kim et al. 2005; Yu et al. 2011). Aldehyde dehydrogenase catalyzes the oxidation of aldehydes to their corresponding carboxylic acids and requires NAD or NADP as a co-factor (Sunkar et al. 2003). Moreover, our metabolomics data showed slight decreases in three intermediates of the tricarboxylic acid cycle (TCA cycle), 2-oxoglutarate, malate and fumarate, after salt treatment (Fig. 7). This result is consistent with the metabolic profiles of the *S. salsa* response to salinity (Wu et al. 2011). The down-regulation in these metabolites indicated that salinity induced disturbances in the TCA cycle. Taken together, these results might indicate that the carbohydrate metabolic pathways related to energy supply were inhibited by salt stress in *S. corniculata*.

We also found that two key enzymes involved in the glycolysis pathway glyceraldehyde-3-phosphate dehydrogenase (spot 330) and fructose-bisphosphate aldolase (spot 737) decreased in abundance following $NaHCO_3$ treatment in *S. corniculata*. Glyceraldehyde-3-phosphate dehydrogenase catalyzes the conversion of glyceraldehyde-3-phosphate to 1, 3-diphosphoglycerate. Fructose-bisphosphate aldolase is a type of lyase that catalyzes the interconversion of 1, 6-diphosphate, dihydroxyacetone phosphate and glyceraldehyde-3-phosphate. Being in a different situation from *P. tenuiflora*, these two enzymes were all induced under alkali stress (Yu et al. 2013). Interestingly, our study demonstrates that the content of four intermediates in TCA cycle, 2-oxoglutarate, malate, fumarate and succinate were increased by more than four-fold (Fig. 7). In addition, a decrease in sucrose and increase in glucose and fructose were observed, indicating an up-regulation of the conversion of sucrose to glucose and fructose was induced by alkalinity exposure. Combined with the heightened TCA cycle activity, these results suggest that the degradation of sucrose may supply more substrate for the TCA cycle to generate extra energy, which is beneficial to *S. corniculata* under alkali stress. This result implies that the intensity of the interaction between the sugar metabolism and the TCA cycle is strengthened by alkalinity.

Photosynthesis

The primary step in energy production in the biosphere, photosynthesis, is inhibited by salt and alkali stress (Ma et al. 1997; Yang et al. 2009). Photosynthetic capacity has been observed to be much lower under both salt and alkali stresses than in control plants in the glycophytes wheat and barley, and the inhibition was more severe under alkali stress than salt stress (Yang et al. 2008c, 2009). However, the situation is different in the halophyte *Chloris virgata*, whose photosynthetic properties were not influenced by salt and alkali treatment below 160 mM (Yang et al. 2008a). Our previous study analyzed the photosynthesis and chlorophyll fluorescence parameters of *S. corniculata* seedlings under different concentrations of salt or alkali stress, and the results indicated that the photosynthesis of *S. corniculata* seedlings exhibited no significant difference under low salinity stress compared with the control plants, whereas it was inhibited by high salinity and alkalinity (Wei et al. 2012). Similarly, Fv/fm, Fv'/Fm', qL, and φPSII were not affected by salt stress in *S. salsa* and *S. aegyptiaca* of the *Suaeda* plants (Lu et al. 2003; Askari et al. 2006).

In this work, we found two and three differentially expressed proteins related to photosynthesis in *S. corniculata* response to salt and alkali stress, respectively. Chloroplast RNA binding protein (spot 1015, spot 183 and 1008) was down-regulated by both treatments. Chloroplast RNA binding protein (cRBP) represents good candidate for mediating the function of nucleus-encoded factors which mainly regulate

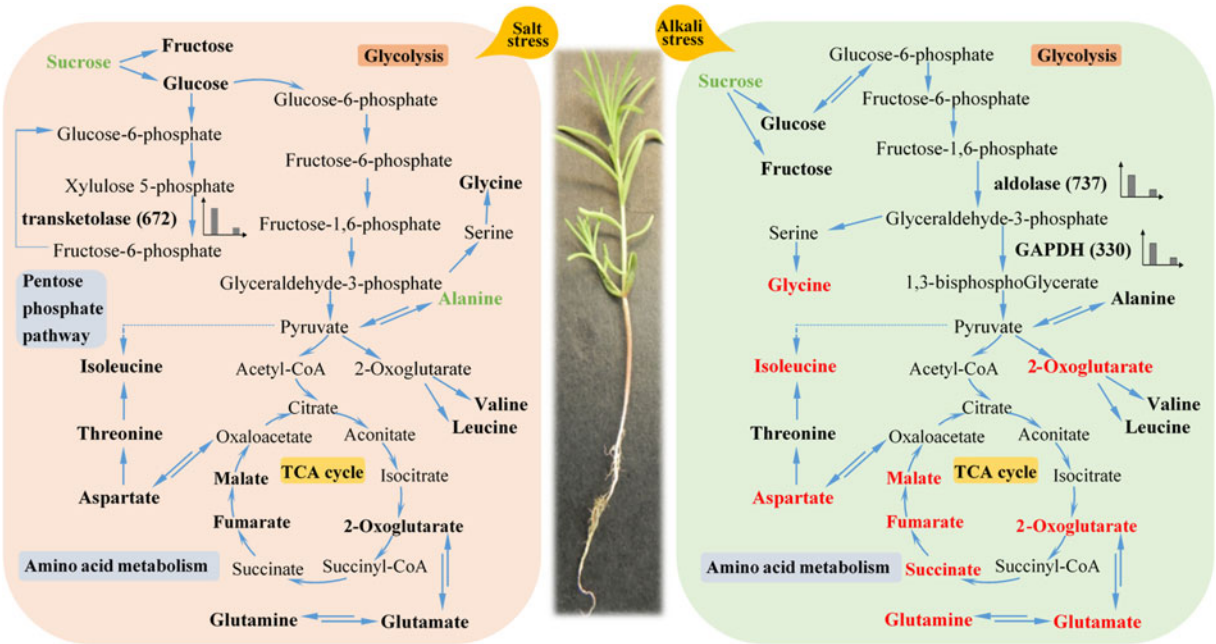

Fig. 7 Main biological pathways responses to salt and alkali stress in *S. corniculata*. The differentially expressed proteins are marked in bold, and the changes in expression abundance of each protein are plotted in a histogram. The up-regulated metabolites are marked with bold in red and the down-regulated metabolites in green. GAPHD, glyceraldehyde 3-phosphate dehydrogenase. TCA cycle, tricarboxylic acid cycle

chloroplast gene expression at the posttranscriptional level (Nickelsen 2003). In the halophyte *Mesembryanthemum crystallinum*, cRBP was increased under salt stress at the transcript level, but it is unknown whether the protein abundance was affected (Breiteneder et al. 1994). Interestingly, we also found that the RuBisCO large subunit-binding protein subunit beta (spot 572) was up-regulated by alkali treatment. This protein binds non-covalently to rubisco large subunits and is implicated in the assembly of RuBisCO in higher plant chloroplasts (Musgrove and Ellis 1986). In a large-scale expressed sequence tag analysis of halophyte *Tamarix hispid* to examine salinity-alkali stress responses, the abundance of RuBisCO was significantly up-regulated under $NaHCO_3$ stress for 52 h (Gao et al. 2008). Proteomics analysis of *P. tenuiflora* showed that RuBisCO was suppressed after either salt or alkali stress (Yu et al. 2011, 2013). In contrast, the RuBisCO assembling protein was induced by alkali stress in *S. corniculata* which could positively impact the expression of RuBisCO. This result is consistent with our previous findings that the leaf intercellular CO_2 levels in *S. corniculata* increased under $NaHCO_3$ stress (Wei et al. 2012), which implied that this stress might enhance the CO_2 fixation by RuBisCO and improve the photosynthetic capacity. These results suggested that the modulation of photosynthesis might contribute to the ability of *S. corniculata* to cope with alkalinity.

Protein processing and amino acid metabolism

Proteomics studies revealed that the expression of many components of protein synthesis machinery are altered under salt stress conditions and suggested that protein synthesis plays a vital role in abiotic stress adaptation (Wang et al. 2008; Witzel et al. 2009; Pang et al. 2010). Our study demonstrated that serine carboxypeptidase (spot 181) and pollen allergen MetE (spot 717),respectively related to protein processing and amino acid metabolism were down-regulated under salt stress. Metabolomics analysis demonstrated that alanine which was the cross center of amino acid metabolism was decreased in *S. corniculata* with salinity exposure (Fig. 7). This results is consistent with findings in *S. salsa* and *Thellungiella salsuginea* (Lugan et al. 2010; Wu et al. 2012). These results suggest that salinity restrain amino acid metabolism in *S. corniculata* which may lead to a reduction of organic acids because it would lessen the capacity of osmotic adjustment under salt stress.

In alkali treated plants, we observed that ATP-dependent zinc metalloprotease FTSH 2 (spot 642) was more abundant in *S. corniculata*. It has been reported that FTSH is the only membrane-bound ATP-dependent protease that functions in the efficient degradation of proteins and is also involved in protection against environmental stress (Yoshioka et al. 2006). The up regulation of ATP-dependent zinc metalloprotease FTSH in our study may indicate that it can help to degrade the incorrectly folded proteins, which may be a self-protection mechanism in *S. corniculata* response to alkali stress. In support of this possibility, we also found that amino acids including glycine, isoleucine, glutamate, glutamine and aspartate were highly accumulated in *S. corniculata* under alkali stress (Fig. 7). The high level organic acids may compensate for the ionic imbalance induced by alkalinity and improve the osmotic adjustment through the accumulation of free amino acids for coping with alkali stress in *S. corniculata*.

Other

The accumulation of organic osmolytes, such as proline, glycine betaine, and sugar alcohols, is essential in maintaining the low intracellular osmotic potential of plants and in preventing the harmful effects of salinity stress (Verslues et al. 2006). According to our study, betaine and choline were highly accumulated in *S. corniculata*, with significant induction by alkali stress. The conversion of choline to betaine aldehyde by choline monooxygenase is a key step in the betaine biosynthesis pathway (Peel et al. 2010). The accumulation both of betaine and choline indicates the enhancement of betaine biosynthesis. In accordance with this finding, we also found that soluble sugars including fructose and glucose were more abundant in *S. corniculata* under alkali stress than in salt-treated plants. Taken together, these findings account for the positive modulation of osmotic adjustment in *S. corniculata*, which may be a key regulatory mechanism in *S. corniculata* to withstand alkalinity.

Conclusions

We performed integrated proteomics and metabolomics analyses to examine the different molecular mechanisms in the *S. corniculata* response to salt and alkali stress in this study. Our observations successfully identified, 22 proteins and 19 metabolites involved in several metabolic pathways. The down-regulation of certain key enzymes and intermediates demonstrates that carbohydrate metabolism, photosynthesis and the TCA cycle, all related to energy supply were inhibited by salt stress. The higher abundance of monosaccharides and intermediates of the TCA cycle accumulated in *S. corniculata* under alkali treatment provided more energy source for the plant to counteract the adverse effects of alkalinity. The levels of free amino acids exhibited contrasting changes in response to salt and alkali stress. Compared with salt treatment, the accumulation of organic osmolytes was much higher in alkali-treated plants. These results revealed that different regulatory mechanisms were used in the halophyte *S. corniculata* to adapt to salt and alkali stress. In particular, the up-regulation of energy metabolism and higher accumulation of organic osmolytes indicate that *S. corniculata* possess high pH resistance to alkali stress.

Acknowledgments This work was supported by the Fundamental Research Funds for the Central Universities (DL12CA01), the National Natural Science Foundation of China (No. 31300305), the Research Fund for the Doctoral Program of Higher Education and the Postdoctoral Funding of Heilongjiang Province.

References

Askari H, Edqvist J, Hajheidari M, Kafi M, Salekdeh GH (2006) Effects of salinity levels on proteome of *Suaeda aegyptiaca* leaves. Proteomics 6:2542–2554. doi:10.1002/pmic.200500328

Ayarpadikannan S, Chung E, Cho CW, So HA, Kim SO, Jeon JM, Kwak MH, Lee SW, Lee JH (2012) Exploration for the salt stress tolerance genes from a salt-treated halophyte, *Suaeda asparagoides*. Plant Cell Rep 31:35–48. doi:10.1007/s00299-011-1137-4

Breiteneder H, Michalowski CB, Bohnert HJ (1994) Environmental stress-mediated differential 3′ end formation of chloroplast RNA-binding protein transcripts. Plant Mol Biol 26:833–849

Chen YZ, Pang QY, Dai SJ, Wang Y, Chen SX, Yan XF (2011) Proteomic identification of differentially expressed proteins in *Arabidopsis* in response to methyl jasmonate. J Plant Physiol 168:995–1008. doi:10.1016/j.jplph.2011.01.018

Flowers TJ, Colmer TD (2008) Salinity tolerance in halophytes. New Phytol 179:945–963. doi:10.1111/j.1469-8137.2008.02531.x

Flowers TJ, Ward ME, Hall JL (1976) Salt tolerance in the halophyte *Suaeda maritima*: some properties of malate

dehydrogenase. Phil Trans R Soc Lond B 273:523–540. doi:10.1098/rstb.1976.0029

Gao CQ, Wang YC, Liu GF, Yang CP, Jiang J, Li HY (2008) Expression profiling of salinity-alkali stress responses by large-scale expressed sequence tag analysis in Tamarix hispid. Plant Mol Biol 66:245–258. doi:10.1007/s11103-007-9266-4

Guan B, Yu JB, Lu ZH, Japhet W, Chen XB, Xie WJ (2010) Salt tolerance in two *Suaeda* species: seed germination and physiological responses. Asian J Plant Sci 9:194–199

Guan B, Yu JB, Wang XH, Fu YQ, Kan XY, Lin QX, Han GX, Lu ZH (2011) Physiological responses of halophyte *Suaeda salsa* to water table and salt stresses in coastal wetland of Yellow River Delta. Clean-Soil, Air, Water 39:1029–1035

Guo R, Shi LX, Yang YF (2009) Germination, growth, osmotic adjustment and ionic balance of wheat in response to saline and alkaline stresses. Soil Sci Plant Nutr 55:667–679. doi:10.1111/j.1747-0765.2009.00406.x

Guo QL, Shi DC, Wang DL (2010) The key physiological response to alkali stress by the alkali-resistant halophyte *puccinellia tenuiflora* is the accumulation of large quantities of organic acids and into the rhyzosphere. J Agron Crop Sci 196:123–135. doi:10.1111/j.1439-037X.2009.00397.x

Han N, Shao Q, Bao HY, Wang BS (2011) Cloning and characterization of a Ca^{2+}/H^{+} antiporter from halophyte *Suaeda salsa* L. Plant Mol Biol Rep 29:449–457. doi:10.1007/s11105-010-0244-7

Henkes S, Sonnewald U, Badur R, Flachmann R, Stitt M (2001) A small decrease of plastid transketolase activity in antisense tobacco transformants has dramatic effects on photosynthesis and phenylpropanoid metabolism. Plant Cell 13:535–551. doi:10.1105/tpc.13.3.535

Ji CL, Wu HF, Wei L, Zhao JM, Lu HJ, Yu JB (2013) Proteomic and metabolomic analysis of earthworm *Eisenia fetida* exposed to different concentrations of 2,2′,4,4′-tetrabromodiphenyl ether. J Proteome 91:405–415. doi:10.1016/j.jprot.2013.08.004

Kawanabe S, Zhu TC (1991) Degeneration and conservation of *Aneurolepidium chinense* grassland in Northern China. J Jap Grassland Sci 37:91–99

Khan AM, Ungar IA (1998) Germination of the salt tolerant shrub *Suaeda fruticosa* from Pakistan: salinity and temperature responses. Seed Sci Technol 26:657–667

Kim DW, Rakwal R, Agrawal GK, Jung YH, Shibato J, Jwa NS, Iwahashi Y, Iwahashi H, Kim DH, Shim IS, Usui K (2005) A hydroponic rice seedling culture model system for investigating proteome of salt stress in rice leaf. Electrophoresis 26: 4521–4539. doi:10.1002/elps.200500334

Li XY, Liu JJ, Zhang YT, Lin JX, Mu CS (2009) Physiological responses and adaptive strategies of wheat seedlings to salt and alkali stresses. Soil Sci Plant Nutr 55:680–684. doi:10.1111/j.1747-0765.2009.00408.x

Li W, Zhang CY, Lu QT, Wen XG, Lu CM (2011) The combined effect of salt stress and heat shock on proteome profiling in *Suaeda salsa*. J Plant Physiol 168:1743–1752. doi:10.1016/j.jplph.2011.03.018

Liu L, Wang Y, Wang N, Dong YY, Fan XD, Liu XM, Yang J, Li HY (2011a) Cloning of a vacuolar H^{+}-pyrophosphatase gene from the halophyte *Suaeda corniculata* whose heterologous overexpression improves salt, saline-alkali and drought tolerance in *Arabidopsis*. J Integr Plant Biol 53:731–742. doi:10.1111/j.1744-7909.2011.01066.x

Liu XL, Zhang LB, You LP, Wu HF, Zhao JM, Cong M, Li F, Wang Q, Li LZ, Li CH, Han GX, Wang GM, Xia CH, Yu JB (2011b) Metabolomic study on the halophyte *Suaeda salsa* in the Yellow River Delta. Clean-Soil, Air, Water 39:720–727. doi:10.1002/clen.201000515

Lu JM, Li JD (1994) The anatomical study in *Suaeda Corniculata* (C.A.M.) Bunge. J Northeast Norm Univ (Natural Science Edition)

Lu CM, Qiu NW, Wang BS, Zhang JH (2003) Salinity treatment shows no effects on photosystem II photochemistry, but increases the resistance of photosystem II to heat stress in halophyte *Suaeda salsa*. J Exp Bot 54:851–860. doi:10.1093/jxb/erg080

Lugan R, Niogret MF, Leport L, Guegan JP, Larher FR, Savoure A, Kopka J, Bouchereau A (2010) Metabolome and water homeostasis analysis of *Thellungiella salsuginea* suggests that dehydration tolerance is a key response to osmotic stress in this halophyte. Plant J 64:215–229. doi:10.1111/j.1365-313X.2010.04323.x

Ma HC, Fung L, Wang SS, Altman A, Hüttermann A (1997) Photosynthetic response of *Populus euphratica* to salt stress. Forest Ecol Manag 93:55–61. doi:10.1016/S0378-1127(96)03943-6

Maathuis FJM, Flowers TJ, Yeo AR (1992) Sodium chloride compartmentation in leaf vacuoles of the halophyte *Suaeda maritima* (L.) Dum. and its relation to tonoplast permeability. J Exp Bot 43:1219–1223

Munns R (2002) Comparative physiology of salt andwater stress. Plant Cell Environ 25:239–250. doi:10.1046/j.0016-8025.2001.00808.x

Munns R, Tester M (2008) Mechanisms of salinity tolerance. Annu. Rev Plant Biol 59:651–681. doi:10.1146/annurev.arplant.59.032607.092911

Musgrove JE, Ellis RJ (1986) The rubisco large subunit binding protein. Philos Trans R Soc B 312:419–428

Nickelsen J (2003) Chloroplast RNA-binding proteins. Curr Genet 43:392–399. doi:10.1007/s00294-003-0425-0

Pang CH, Zhang SJ, Gong ZZ, Wang BS (2005) NaCl treatment markedly enhances H_2O_2-scavenging system in leaves of halophyte *Suaeda salsa*. Physiol Plant 125:490–499. doi:10.1111/j.1399-3054.2005.00585.x

Pang QY, Chen SX, Dai SJ, Chen YZ, Wang Y, Yan XF (2010) Comparative proteomics of salt tolerance in *Arabidopsis thaliana* and *Thellungiella halophila*. J Proteome Res 9: 2584–2599. doi:10.1021/pr100034f

Peel GJ, Mickelbart MV, Rhodes D (2010) Choline metabolism in glycine betaine accumulating and non-accumulating nearisogenic lines of *Zea mays* and *Sorghum bicolor*. Phytochemistry 71:404–414. doi:10.1016/j.phytochem.2009.11.002

Qi CH, Chen M, Song J, Wang BS (2009) Increase in aquaporin activity is involved in leaf succulence of the euhalophyte *Suaeda salsa*, under salinity. Plant Sci 176:200–205. doi:10.1016/j.plantsci.2008.09.019

Qiu NW, Chen M, Guo JR, Bao HY, Ma XL, Wang BS (2007) Coordinate up-regulation of V-H^{+}-ATPase and vacuolar Na^{+}/H^{+} antiporter as a response to NaCl treatment in a C_3 halophyte *Suaeda salsa*. Plant Sci 172:1218–1225. doi:10.1016/j.plantsci.2007.02.013

Shao QL, Li YJ (1998) Well Development of *Suaeda salsa*. Plants 3:12

Shi DC, Zhao KF (1997) Effects of NaCl and Na_2CO_3 on growth of *Puccinellia tenuiflora* and on present state of mineral elements in nutrient solution. Acta Pratacu Sin 6:51–61

Song J, Feng G, Tian C, Zhang FS (2006) Osmotic adjustment traits of *Suaeda physophora*, *Haloxylon ammodendron* and *Haloxylon persicum* in field or controlled conditions. Plant Sci 170:113–119. doi:10.1016/j.plantsci.2005.08.004

Song J, Chen FG, Jia YH, Wang BS, Zhang FS (2009) Effect of salinity on growth, ion accumulation and the roles of ions in osmotic adjustment of two populations of *Suaeda salsa*. Plant Soil 314:133–141. doi:10.1007/s11104-008-9712-3

Sunkar R, Bartels D, Kirch HH (2003) Overexpression of a stress-inducible aldehyde dehydrogenase gene from *Arabidopsis thaliana* in transgenic plants improves stress tolerance. Plant J 35:452–464. doi:10.1046/j.1365-313X.2003.01819.x

Verslues PE, Agarwal M, Katiyar-Agarwal S, Zhu JH, Zhu JK (2006) Methods and concepts in quantifying resistance to drought, salt and freezing, abiotic stresses that affect plant water status. Plant J 45:523–539. doi:10.1111/j.1365-313X.2005.02593.x

Wallender WW, Tanji KK (1990) Agricultural salinity assessment and management. Am Soc Civ Eng. New York pp:1–112. ISBN: 978-0-7844-1169-8

Wang BS, Lüttge U, Ratajczak R (2001) Effects of salt treatment and osmotic stress on V-ATPase and V-PPase in leaves of the halophyte *Suaeda salsa*. J Exp Bot 52:2355–2365. doi:10.1093/jexbot/52.365.2355

Wang BS, Lüttge U, Ratajczak R (2004) Specific regulation of SOD isoforms by NaCl and osmotic stress in leaves of the C_3 halophyte *Suaeda salsa* L. J Plant Physiol 161:285–293. doi:10.1078/0176-1617-01123

Wang XQ, Yang PF, Gao Q, Liu XL, Kuang TY, Shen SH, He YK (2008) Proteomic analysis of the response to high-salinity stress in *Physcomitrella patens*. Planta 228:167–177. doi:10.1007/s00425-008-0727-z

Wei L, Pang QY, Zhang AQ, Guo J, Yan XF (2012) Effects of salt and alkali stresses on photosynthetic characteristics of *Suaeda corniculata* seedlings. J Northeast For Univ 40:32–35

Wetson AM, Flowers TJ (2010) The effect of saline hypoxia on growth and ion uptake in *Suaeda maritima*. Funct Plant Biol 37:646–655. doi:10.1071/FP09270

Witzel K, Weidner A, Surabhi GK, Borner A, Mock HP (2009) Salt stress-induced alterations in the root proteome of barley genotypes with contrasting response towards salinity. J Exp Bot 60:3545–3557. doi:10.1093/jxb/erp198

Wu HF, Liu XL, You LP, Zhang LB, Yu JB, Zhou D, Zhao JM, Feng JH (2011) Salinity-induced effects in the halophyte *Suaeda salsa* using NMR-based metabolomics. Plant Mol Biol Rep 30:590–598. doi:10.1007/s11105-011-0368-4

Wu HF, Liu XL, You LP, Zhang LB, Zhou D, Feng JH, Zhao JM, Yu JB (2012) Effects of salinity on metabolic profiles, gene expressions, and antioxidant enzymes in halophyte *Suaeda salsa*. J Plant Growth Regul 31:332–341. doi:10.1007/s00344-011-9244-6

Wu HF, Liu XL, Zhang XY, Ji CL, Zhao JM, Yu JB (2013) Proteomic and metabolomic responses of clam *Ruditapes philippinarum* to arsenic exposure under different salinities. Aquat Toxicol 136-137:91–100. doi:10.1016/j.aquatox.2013.03.020

Xu L (2004) Methods of chemometrics. Science Press, Beijing, pp. 221–227

Yang CW, Chong JN, Li CY, Kim C, Shi DC, Wang DL (2007) Osmotic adjustment and ion balance traits of an alkali resistant halophyte *Kochia sieversiana* during adaptation to salt and alkali conditions. Plant Soil 294:263–276. doi:10.1007/s11104-007-9251-3

Yang CW, Jianaer A, Li CY, Shi DC, Wang DL (2008a) Comparison of the effects of salt-stress and alkali-stress on photosynthesis and energy storage of an alkali-resistant halophyte *Chloris virgata*. Photosynthetica 46:273–278

Yang CW, Shi DC, Wang DL (2008b) Comparative effects of salt stress and alkali stress on growth, osmotic adjustment and ionic balance of an alkali resistant halophyte *Suaeda glauca* (Bge). Plant Growth Regul 56:179–190. doi:10.1007/s10725-008-9299-y

Yang CW, Wang P, Li CY, Shi DC, Wang DL (2008c) Comparison of effects of salt and alkali stresses on the growth and photosynthesis of wheat. Photosynthetica 46:107–114

Yang CW, Xu HH, Wang LL, Liu J, Shi DC, Wang DL (2009) Comparative effects of salt-stress and alkali-stress on the growth, photosynthesis, solute accumulation, and ion balance of barley plants. Photosynthetica 47:79–86

Yoshioka M, Uchida S, Mori H, Komayama K, Ohira S, Morita N, Nakanishi T, Yamamoto Y (2006) Quality control of photosystem II. Cleavage of reaction center D1 protein in spinach thylakoids by FtsH protease under moderate heat stress. J Biol Chem 281:21660–21669. doi:10.1074/jbc.M602896200

Yu JJ, Chen SX, Zhao Q, Wang T, Yang CP, Diaz C, Sun GR, Dai SJ (2011) Physiological and proteomic analysis of salinity tolerance in *Puccinellia tenuiflora*. J Proteome Res 10:3852–3870. doi:10.1021/pr101102p

Yu JJ, Chen SX, Wang T, Sun GR, Dai SJ (2013) Comparative Proteomic Analysis of *Puccinellia tenuiflora* Leaves under Na_2CO_3 Stress. Int J Mol Sci 14:1740–1762. doi:10.3390/ijms14011740

Zhang HY, Zhao KF (1998) Effects of salt and water stresses on osmotic adjustment of *Suaeda salsa* seedlings. Acta Bot Sin 40:56–61

Zhang L, Ma XL, Zhang Q, Ma CL, Wang PP, Sun YF, Zhao YX, Zhang H (2001) Expressed sequence tags from a NaCl-treated *Suaeda salsa* cDNA library. Gene 267:193–200. doi:10.1016/S0378-1119(01)00403-6

Zheng HY, Li JD (1999) Form and dynamic trait of halophyte community. In: Zheng HY (ed) Saline Plants in Songnen Plain and Restoration of Alkaline-Saline Grass. Science Press, Beijing, pp. 137–138

Zhu JK (2001) Plant salt tolerance. Trends Plant Sci 6:66–71. doi:10.1016/S1360-1385(00)01838-0